

The Detectability of Orphan Afterglows

Ehud Nakar & Tsvi Piran

Racah Institute for Physics, The Hebrew University, Jerusalem 91904, ISRAEL

Jonathan Granot

Institute for Advanced Studies, Princeton, NJ 08540, USA

ABSTRACT

The realization that GRBs release a constant amount of energy implies that the post jet-break afterglow evolution would be largely universal. For a given redshift all afterglows should be detected up to a fixed observer angle. We estimate the observed magnitude and the implied detectability of orphan afterglows. We show that for reasonable limiting magnitudes ($m_{lim} = 25$) orphan afterglows would typically be detected from small ($\sim 10^\circ$) angles away from the GRB jet axis. A detected orphan afterglow would generally correspond to a “near-miss” of the GRB whose jet was pointing just slightly away from us. With our most optimistic parameters we expect 15 orphan afterglows in the SDSS and 35 transients in a dedicated 2m class telescope operating full time for a year in an orphan afterglow search. The rate is smaller by a factor of 15 for our “canonical” parameters. We show that for a given facility an optimal survey should be shallower, covering larger area rather than deeper. The limiting magnitude should not be, however, lower than 25th as in this case more transient from on-axis GRBs will be discovered than orphan afterglows. About 15% of the transients could be discovered with a second exposure of the same area provided that it follows after 3, 4 and 8 days for $m_{lim} = 23, 25$ and 27.

-

1. Introduction

The realization that GRBs are beamed with a rather narrow opening angles, while the following afterglow could be observed over a wider angular range, led immediately to the search for orphan afterglows: afterglows which are not associated with observed prompt GRB emission. Rhoads (1997) was the first to suggest that observations of orphan afterglows would enable us to estimate the opening angles and the true rate of GRBs. An expanding jet with an opening angle θ_j , behaves, as long as its Lorentz factor $\gamma > \theta_j^{-1}$, as if it is a part of a spherical shell (Piran, 1994). As it slows down and reaches $\gamma \approx \theta_j^{-1}$ the jet quickly expands laterally (Rhoads, 1999) producing a pronounced break in its light curve. As time progresses it can be observed over wider and wider observing angles, θ_{obs} . Dalal et al. (2002) have pointed out that as the post jet-break afterglow

light curves decay quickly most orphan afterglow will be dim and hence undetectable. They also suggest that the maximal observing angle, θ_{max} , of an orphan afterglow will be a constant factor times θ_j . Hence the ratio of observed orphan afterglows, R_{orph}^{obs} , to that of GRBs, R_{GRB}^{obs} , will not tell us much about the opening angles of GRBs and the true rate of GRBs, R_{GRB}^{true} .

The observation that GRBs have a constant amount of total energy (Piran et al, 2001; Panaitescu and Kumar 2001; Frail et al., 2001) and that the observed variability in the apparent luminosity arises mostly from variation in the jet opening angles leads to a remarkable result: The post jet-break afterglow light curve is universal (Granot et al., 2002). We calculate this universal post jet-break light curve, using both first principle considerations and a calibration from the observed afterglows of GRB990510 (Harrison et al., 1999; Stanek et al., 1999), and GRB000926 (Harrison et al., 2001). Using this light curve we estimate the maximal flux at an observing angle θ_{obs} from the jet axis. Using this flux we estimate the total number of orphan afterglows that can be observed given a limiting magnitude and the distribution of these orphan afterglows as a function of θ_{obs} and the redshift, z .

The assumption that the total energy is constant implies that orphan afterglow will be detected roughly up to a constant observing angle (independent of θ_j). In this case $R_{orph}^{obs} \propto R_{GRB}^{true}$ and can teach us about the distribution of θ_j (Granot et al. 2002). We show that this result holds for the case of strong beaming (small jet opening angles and large beaming factors).

We describe our analytic model and the phenomenological fits to the observations in §2. We present our estimates for the observed rate of orphan afterglows in §3. We stress that these are idealized optimistic estimates that do not consider various observational obstacles. In §4 we compare our estimates for the expected rate of orphan afterglows with the capabilities of several surveys.

2. The Model

Consider an adiabatic jet with a total energy E and an initial opening angle θ_j . We consider a simple hydrodynamic model for the jet evolution (Rhoads 1999; Sari, Piran & Halpern, 1999). Initially the jet propagates as if it were spherical with an equivalent isotropic energy of $2E/\theta_j^2$:

$$E = (2\pi/3)\theta_j^2 R^3 \gamma^2 n m_p c^2, \quad (1)$$

where n is the ambient number density. The spherical phase continues as long as $\gamma > \theta_j^{-1}$. At this stage the jet expands sideways relativistically in the local frame, with $\gamma = \theta^{-1}$ and adiabaticity implies that

$$E = (2\pi/3)R^3 n m_p c^2, \quad (2)$$

and the radius of the shock remains constant¹. Note that the evolution during this phase is independent of θ_j , whose only role is to determine the time of the jet break. If E and n do not

¹More detailed calculations show that R increases but γ decreases exponentially with R (Rhoads 1999; Piran 2000)

vary from one burst to another then the light curve during this phase will be universal, depending only on the microscopic parameters (the equipartition parameters, $\epsilon_{B,e}$, and the power law index p of the electron distribution) of the specific afterglow. During both phases the observed time is given by:

$$t = (1 + z)R/4c\gamma^2 . \quad (3)$$

Equations 2 and 3 yield that the jet break transition takes place at (Sari, Piran & Halpern, 1999):

$$t_{jet} = 0.7\text{days}(1 + z)(E/10^{51})^{1/3}n_0^{-1/3}(\theta_j/0.1)^2 . \quad (4)$$

Due to relativistic beaming an observer located at θ_{obs} , which is outside the initial opening angle of the jet ($\theta_{obs} > \theta_j$) will (practically) observe the afterglow emission only at t_θ when $\gamma = \theta_{obs}^{-1}$:

$$t_\theta = At_{jet}(\theta_{obs}/\theta_j)^2 , \quad (5)$$

where A is a factor of order unity. At roughly this time the emission is also maximal. From then on it decays in the same way as for an on-axis observer.

The synchrotron slow cooling light curve for the initial (spherical) phase is given by Sari, Piran & Narayan, (1998) and modified by Granot & Sari (2001). Sari Piran & Halpern (1999) give temporal scaling of the maximal flux and the synchrotron and cooling frequencies during the modified hydrodynamic evolution after the jet break. Combining both results [using the Granot & Sari (2001) normalization for the fluxes and typical frequencies] we obtain the universal post jet-break light curve. For the optical band which is usually above the cooling frequency we find:

$$F_\nu(t) = 450\mu\text{Jy} \left[\frac{g(p)}{g(2.2)} \right] 10^{\frac{2.2-p}{4}} \left(\frac{\epsilon_e}{0.1} \right)^{p-1} \left(\frac{\epsilon_B}{0.01} \right)^{\frac{p-2}{4}} n_0^{\frac{-p-2}{12}} \left(\frac{E}{5 \cdot 10^{50}} \right)^{\frac{p+2}{3}} t_{days}^{-p} \left(\frac{\nu}{5 \cdot 10^{14}} \right)^{-p/2} (1+z)^{\frac{2+p}{2}} \left(\frac{D_L}{10^{28}} \right)^{-2} , \quad (6)$$

where D_L is the luminosity distance and $g(p) \equiv 10^{-0.56p}(p - 0.98)[(p - 2)/(p - 1)]^{p-1}$. Using Eq. 5 we obtain the maximal flux that an observer at an θ_{obs} will detect:

$$F_\nu^{max}(\theta_{obs}) = 1600\mu\text{Jy} \frac{g(p)}{g(2.2)} \left(\frac{\epsilon_e}{0.1} \right)^{p-1} \left(\frac{\epsilon_B}{0.01} \right)^{\frac{(p-2)}{4}} n_0^{\frac{(3p-2)}{12}} \left(\frac{E}{5 \cdot 10^{50}} \right)^{\frac{2}{3}} \left(\frac{\theta_{obs}}{0.1} \right)^{-2p} \left(\frac{\nu}{5 \cdot 10^{14}} \right)^{-\frac{p}{2}} (1+z)^{1-p/2} \left(\frac{D_L}{10^{28}} \right)^{-2} . \quad (7)$$

One notices here a very strong dependence on θ_{obs} . The peak flux drops quickly when the observer moves away from the axis. Note also that this maximal flux is independent of the opening angle of the jet, θ_j . Once we know $F_\nu^{max}(\theta_{obs})$ we can estimate, $\theta_{max}(z, m)$, the maximal observing angle at which an afterglow is brighter than a limiting magnitude, m . We then proceed and estimate the total number of orphan afterglows brighter than m .

We can estimate the observed flux using the “canonical” values of the parameters. However, these are uncertain. Alternatively, we can use the observations of the afterglows of GRB990510 (Harrison et al., 1999; Stanek et al., 1999) and of GRB000926 (Harrison et al., 2001), both showing clear jet breaks to obtain an “observational” calibration of $F_\nu(\theta_{obs})$. Using the θ_{obs} dependence found in Eq. 7 we can write:

$$F_\nu(\theta_{obs}) = F_0 f(z) \theta_{obs}^{-2p} , \quad (8)$$

where F_0 is a constant and $f(z) = (1+z)^{1-p/2}(D_L/10^{28})^{-2}$ include all the cosmological effects. If all GRBs are similar with the same total energy, ambient density and microscopic parameters ($\epsilon_{e,B}$ and p) than F_0 is a “universal” constant. However, its value is uncertain. We need the observed flux and θ_{obs} at a certain time to determine F_0 . We use the on-axis observed afterglows at the break time, when an observer at $\theta_{obs} = \theta_j A^{-1/2}$ (for a narrower jet) would observe a similar flux to an on-axis observer (for the observed jet). Using the parameters for GRB990510 from Harrison et. al. 1999 ($\theta_j = 0.08$, $p = 2.1$, and $m_{break} = 20mag$ when m_{break} is the R band magnitude of the afterglow at the break time) and the parameters for GRB000926 from Harrison et. al. 2001 ($\theta_j = 0.1$, $p = 2.2$, and $m_{break} = 20mag$), We find that $F_0(990510) = 0.01\mu Jy$ and $F_0(000926) = 0.03\mu Jy$ and both are rather close to the theoretical estimate with $E_{51} = 0.5$, $n = 1$, $\epsilon_e = 0.1$, $\epsilon_B = 0.005$, $p = 2.2$ which yields $F_0 = 0.014\mu Jy$ and magnitude 20 at the break time (for a burst at $z = 1.6$ with $\theta_j = 0.1$). However, Granot et al. (2002) show, using a more refined simulation of the off-axis light curve (their model II), that when the off-axis light cure ‘join’ the on axis light curve, the off-axis maximal flux is a factor of few less than the on-axis flux. For example a burst at $z = 1$ with $E_{51} = 0.5$, $n = 1$, $\epsilon_e = 0.1$, $\epsilon_B = 0.01$, $p = 2.5$ is estimated in this model at 24th magnitude at $\theta_{obs} = 0.22$. This result corresponds to $F_0 = 0.002\mu Jy$. According to the observations and fact that the off-axis maximal flux is a factor of few less than the on-axis flux we use in the following a “canonical” model of $F_0 = 0.003\mu Jy$ and $p = 2.2$. However, we should keep in mind that there is a large uncertainty (factor of ~ 5) in the absolute value of the flux. This uncertainty does not change θ_{max} that depends on $F_0^{1/2p}$ by a large factor. The overall rate depends, however, almost linearly on F_0 . The total number of observed bursts depends not only on $\theta_{max}^2 \propto F_0^{1/p}$ but also on the duration, t_{obs} which is $\propto \theta_{max}^2$. Together we find that the rate is $\propto F_0^{2/p}$. Fig 1 depicts the R magnitude contour lines for our “canonical” model ($F_0 = 0.003\mu Jy$, $p = 2.2$).

3. Results

For a given limiting magnitude, m , we can calculate now the total number of observed orphan afterglows. For a given z we define $\theta_{max}(z, m)$ such that $23.9 - 2.5 \text{Log}_{10}[F_\nu(\theta_{max}(z, m))] = m$. Fig 1 depicts contour lines of the inverse function $m(\theta_{obs}, z)$ on the (θ, z) plane. We use throughout this paper a “standard” cosmological model with $\Omega_M = 0.3$, $\Omega_\Lambda = 0.7$ and $h = 0.7$.

The rate of observed orphan afterglows (over the whole sky) is:

$$R_{orph} = \int_0^\infty \frac{n(z)}{(1+z)} dV(z) \int_{\theta_j}^{\theta_{max}(z, m)} \theta d\theta = \int_0^\infty \frac{n(z)}{(1+z)} \frac{dv(z)}{dz} dz \frac{\theta_{max}(z, m)^2 - \theta_j^2}{2}, \quad (9)$$

where $n(z)$ is the rate of GRBs per unit volume and unit proper time and $dV(z)$ is the differential volume element at redshift z . We assume that the GRB rate is proportional to the SFR and is given by: $n(z) = B 10^{0.75z}$ for $z \leq z_{peak}$ and $n(z) = B 10^{0.75z_{peak}}$ for $z_{peak} < z < 10$. The normalization factor B is found by the condition: $R_{GRB} = f_b R_{GRB}^{obs} = \int_0^{10} n(z) dV/(1+z)$ where f_b is the beaming factor and $R_{GRB}^{obs} = 667 \text{yr}^{-1}$. In the following we consider two star formation rates peaking at

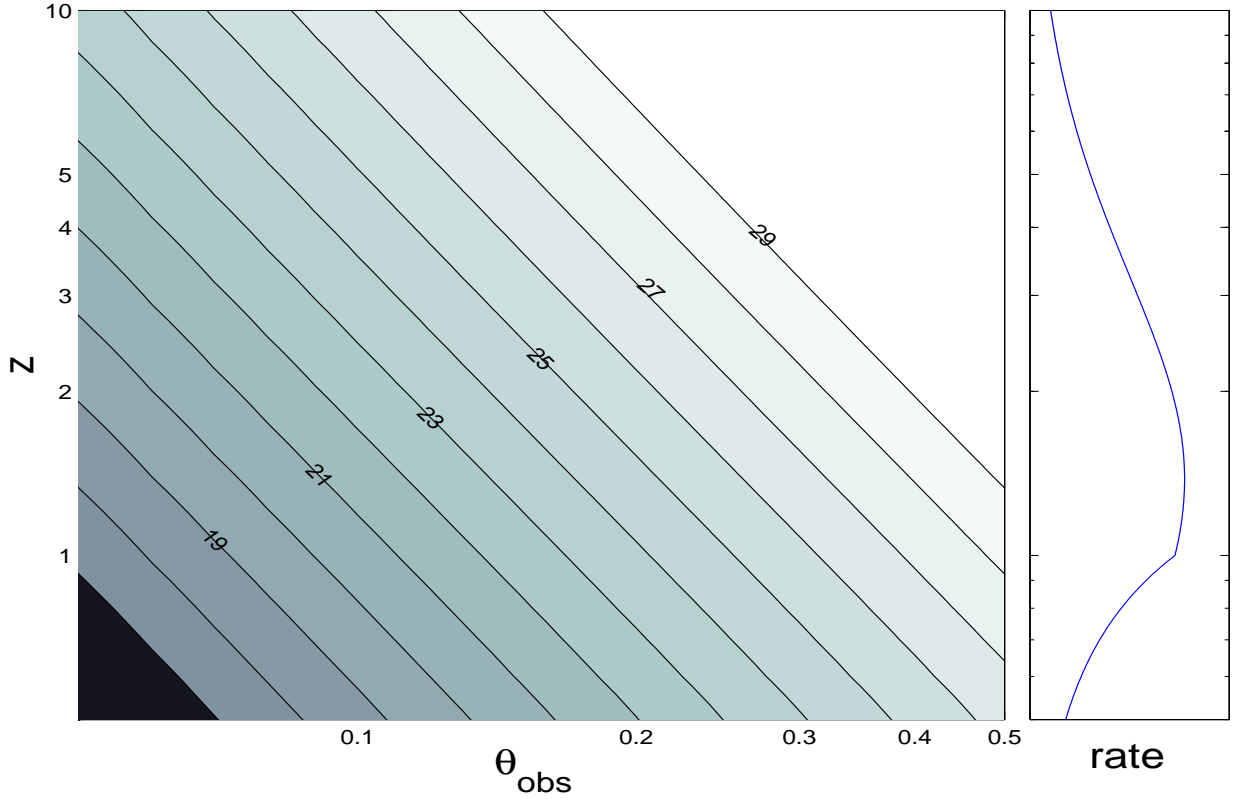


Fig. 1.— Left panel: R magnitude contour lines (from 17- left bottom to 29) for $F_0 = 0.003\mu Jy$. The right panel depicts the GRB rate $n(z)(dV/dz)/(1+z)$ as a function of z (for $z_{\text{peak}} = 1$), as an indication to where we should expect most GRBs. As we plot only the region with $z > 0.5$ the flux depends almost as a power law on the redshift.

$z_{peak} = 1$ and at $z_{peak} = 2$ (Bouwenn, 2002).

Usually the detector’s exposure time is shorter than the time, $t_{obs}(z, \theta, m)$, that the afterglow is brighter than m . Thus, the number of detected orphan afterglows in a single snapshot is:

$$N_{orph} = \int_0^\infty \frac{n(z)}{(1+z)} \frac{dV(z)}{dz} dz \int_{\theta_j}^{\theta_{max}(z,m)} t_{obs}(z, \theta, m) \theta d\theta . \quad (10)$$

The z integrand of Eq. 9 gives the normalized redshift distribution of the observed orphan afterglows (see Fig. 2). This distribution has a broad flat region all the way from $z = 0$ to z_{peak} . It sharply declines above z_{peak} . For a SFR with a higher z_{peak} there are significantly fewer orphan afterglows (see Fig. 4). The function peaks (weakly) at z_{peak} with higher limiting magnitude as more orphan afterglows are observed in this case.

The θ integrand of this equation [with $\theta_{max}(z, m)$ replaced by $z_{max}(\theta, m)$ and integration performed over z] yields the angular distribution (shown in Fig. 3). For 25th limiting magnitude the median observing angle (see lower panel of Fig 3) is 5° - 7° depending on the SFR rate. With lower z_{peak} most GRBs are nearer and hence stronger and detectable to a slightly larger angles. These values are close to the jet opening angles. Most of the observed orphan afterglows with this limiting magnitude will be “near misses” of on-axis events. The $\theta_{max}(z_{peak})$ are significantly larger (10° and 14° respectively). With 27th magnitude the median of the angular distribution moves away out to 12° . This is larger than most GRB beaming angles but still narrow, corresponding only to 2% of the sky.

As the sky coverage of GRB detectors is not continuously 4π it is possible that a GRB pointing towards us will be missed, but its on-axis afterglow will be detected. We compare in Table I the ratio of orphan afterglow to total number (both on-axis and orphan) afterglows. As expected this ratio is large for small jet opening angles and for large limiting magnitudes and it decreases rapidly with increasing θ_j and decreasing m . We see that for an insensitive search ($m_{lim} = 23$) there is a comparable (or even larger) probability that a visual transient is a missed on-axis GRB whose afterglow is detected or an orphan one.

	$m_{lim} = 23$	$m_{lim} = 25$	$m_{lim} = 27$
$z_{peak} = 1, \theta_j = 0.05$	0.76	0.88	0.95
$z_{peak} = 1, \theta_j = 0.1$	0.4	0.64	0.81
$z_{peak} = 1, \theta_j = 0.15$	0.2	0.4	0.64
$z_{peak} = 2, \theta_j = 0.1$	0.2	0.44	0.69

Table I: The ratio of orphan afterglow to total number (both on-axis and orphan) afterglows for different limiting magnitudes and different jet opening angles.

Fig 4 depicts the number of orphan afterglows per square degree in a single exposure as a function of the limiting magnitude. These numbers provide an upper limit to the rate in which

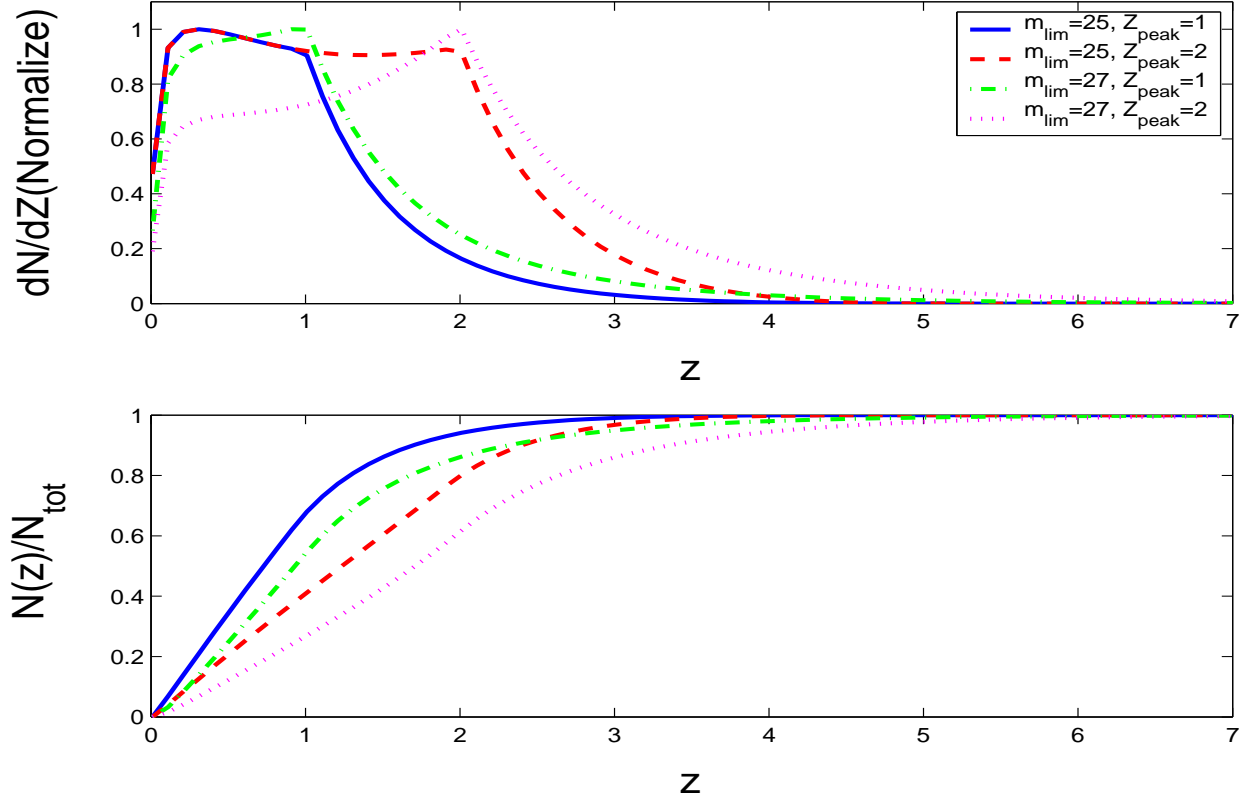


Fig. 2.— Top: The normalized redshift distribution of observed orphan afterglows for $F_0 = 0.003 \mu Jy$, and $\theta_j = 0.1$. The different curves correspond to $m_{\text{lim}} = 25$, $z_{\text{peak}} = 1$ (solid line); $m_{\text{lim}} = 25$, $z_{\text{peak}} = 2$ (dashed line); $m_{\text{lim}} = 27$, $z_{\text{peak}} = 1$ (dashed-dotted line) and $m_{\text{lim}} = 27$, $z_{\text{peak}} = 2$ (dotted line). Bottom: The integrated z distribution.

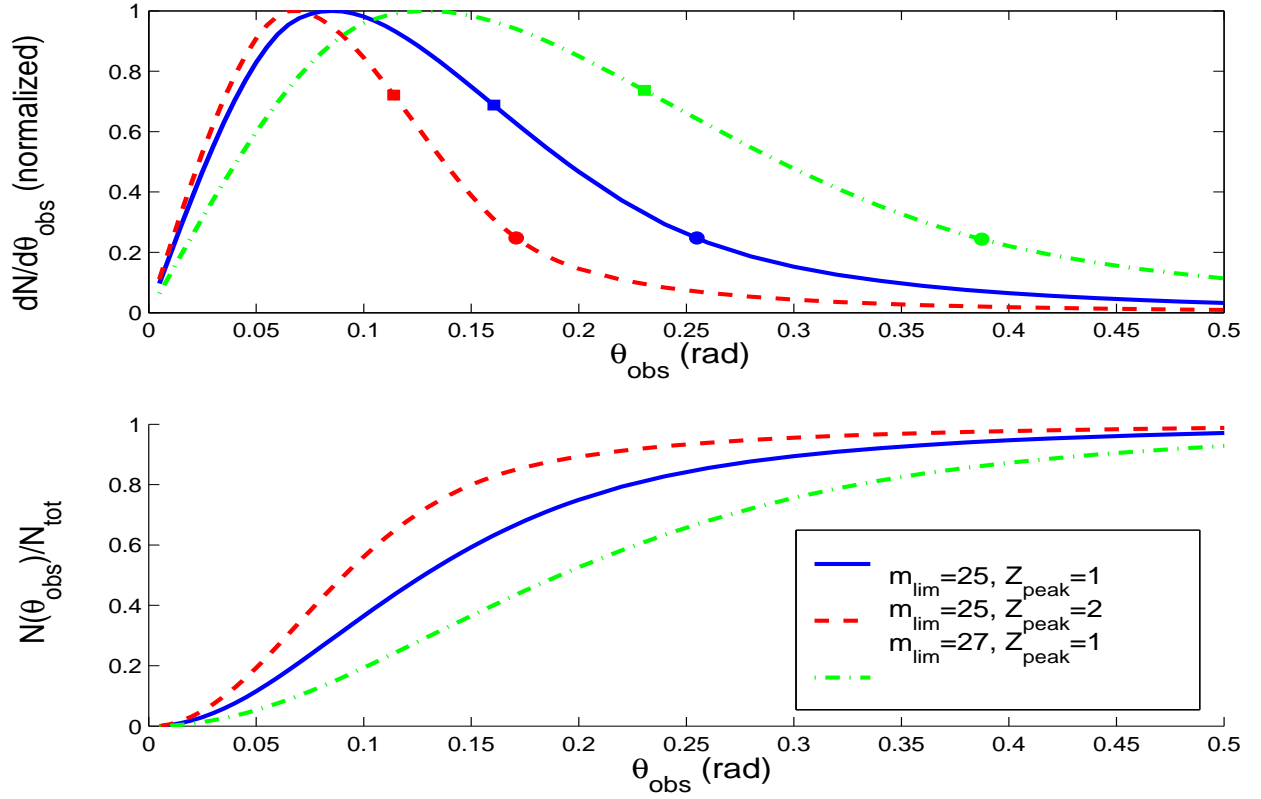


Fig. 3.— Top: The angular distribution of orphan afterglows for three different models: $F_0 = 0.003\mu Jy$, and $m_{\text{lim}} = 25$ and $z_{\text{peak}} = 1$ (solid line); $m_{\text{lim}} = 25$ and $z_{\text{peak}} = 2$ (dashed line); and $m_{\text{lim}} = 27$ and $z_{\text{peak}} = 1$ (dashed-dotted line). The circles depict $\theta_{\text{max}}(z_{\text{peak}}, m)$ and the squares depict $\langle \theta_{\text{obs}} \rangle$. Bottom: the integrated angular distribution for the same models.

orphan afterglows will be recorded as point-like optical transients in any exposure with a given limiting magnitude. These numbers should be considered as upper limits as our estimates do not include effects such as dust extinction or a bright local host galaxy that could made these transients undetectable.

We ask now what will be the optimal strategy for a given observational facility: short and shallow exposures that cover a larger solid angle or long and deep ones over a smaller area. The time to reach a given limiting flux is proportional to one over the flux squared. We can divide now the number density of observed orphan afterglows (shown in Fig 4) by this time factor and obtain the rate per square degree per hour of observational facility. Fig 5 depicts this rate with a calibration to a hypothetical 2m class telescope that reaches a 25th magnitude with one hour exposure. Other telescopes will have another normalization but the trend seen in this figure remains. We find that shallow surveys that cover a large area are preferred over deep ones. Practical advantages of this strategy is that it would be easier to carry out follow up observations with a large telescope on a brighter transient detected in a shallow survey, additionally one can expect that the number of spurious transients will be smaller in a shallower survey. However, if one wishes to detect orphan afterglows one should still keep the surveys at a limiting magnitude of ~ 25 as for smaller magnitude more on-axis transients will be detected than orphan afterglows (see Table I).

The number density of orphan afterglow transients, given by Eq. 10 and depicted in Fig. 4 gives an indication of the number of single event recorded above a limiting magnitude. However, a minimal (very optimistic) requirement for an identification that the transient indeed corresponded to an afterglow would be a second following detection with a decrease by, say 1 magnitude. We estimate the rate of a double detection of this nature by an afterglow search with a limiting magnitude m_{lim} and a time delay dT_{obs} between the two exposures to the same region in the sky. We consider as an identification a detection of a transient in one exposure and a second detection after time dT_{obs} in which the transient has decayed more than one magnitude but is still above the limiting magnitude of the survey. This is of course an idealized situation and we do not consider realistic observational problems (like weather etc..) which may make the detection rate lower. Not surprisingly the ratio of a double detection to a single detection depends on the time delay, dT_{obs} (see Fig. 6). The optimal delay is, not surprisingly, the time in which an afterglow from z_{peak} and with m_{lim} decays by one magnitude: $dT_{obs} = 3$ days for $m_{lim} = 23$, $dT_{obs} = 4$ days for $m_{lim} = 25$ and $dT_{obs} = 8$ days for $m_{lim} = 27$. With this optimal choice about 20% for $m_{lim} = 27$ and 12% for $m_{lim} = 23$ of the detected transients will be detected in a second exposure. Note however, that the curve becomes narrower for low magnitudes, making the exact timing of the second exposure more critical. Deeper surveys are less sensitive to the choice of the time delay.

It is interesting to compare the rate of observed orphan afterglow to the true GRB rate. We consider an idealized situation in which we observe all orphan afterglows above m_{lim} with a 4π coverage. We see that for strong beaming (narrow beaming angles and a large beaming factor) this ratio converges to a constant value (which depends, however, on the specific model). Thus in this case it is possible to estimate the true GRB rate from a determination of the orphan afterglow rate.

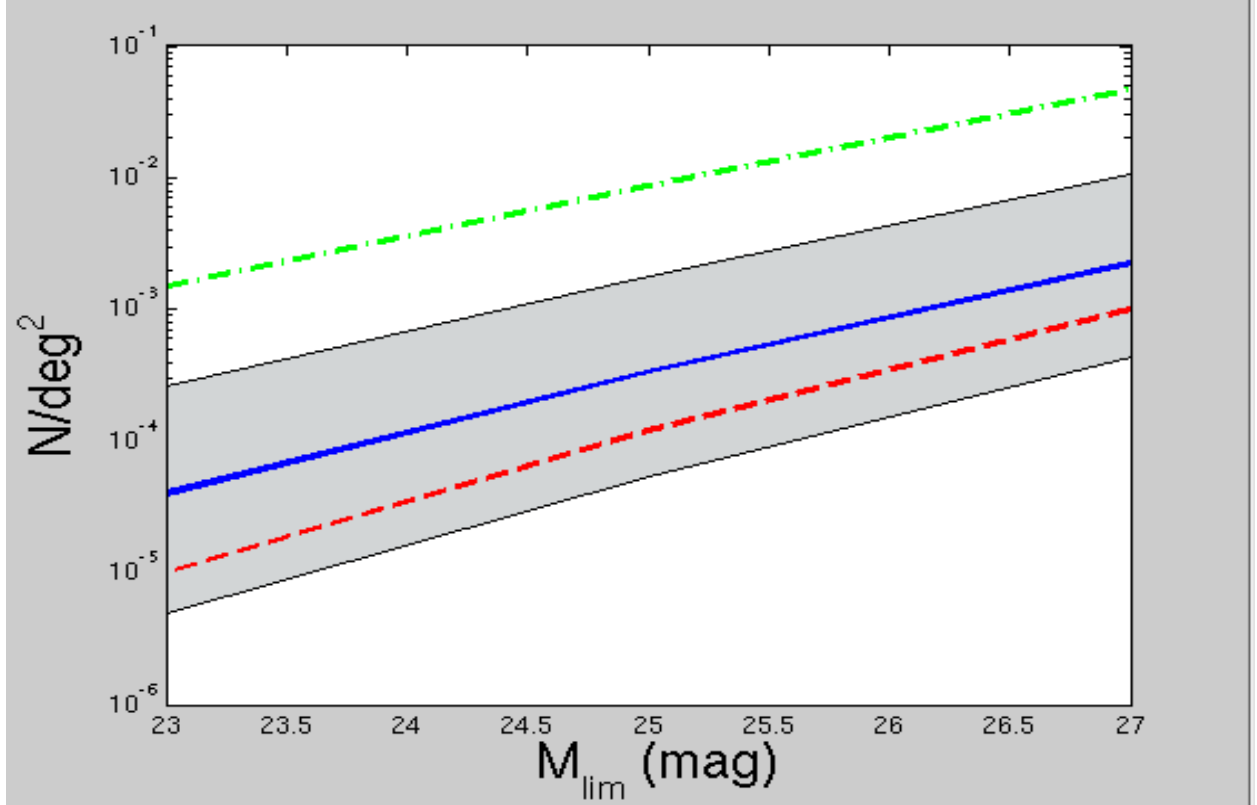


Fig. 4.— The number of observed orphan afterglows per square degree in a single exposure. We consider three different models: The solid line corresponds to our “canonical” normalization ($F_0 = 0.003 \mu\text{Jy}$, $z_{\text{peak}} = 1$ and $\theta_j = 0.1$). The gray area around this line corresponds an uncertainty by a factor of 5 in this normalization ($0.0006 \mu\text{Jy} < F_0 < 0.015 \mu\text{Jy}$). The dashed-dotted line corresponds to our most optimistic model $F_0 = 0.015 \mu\text{Jy}$, $\theta_j = 0.05$ (as seen in the narrowest beams). The dashed line corresponds to at $z_{\text{peak}} = 2$ and the rest of the “canonical” model parameters.

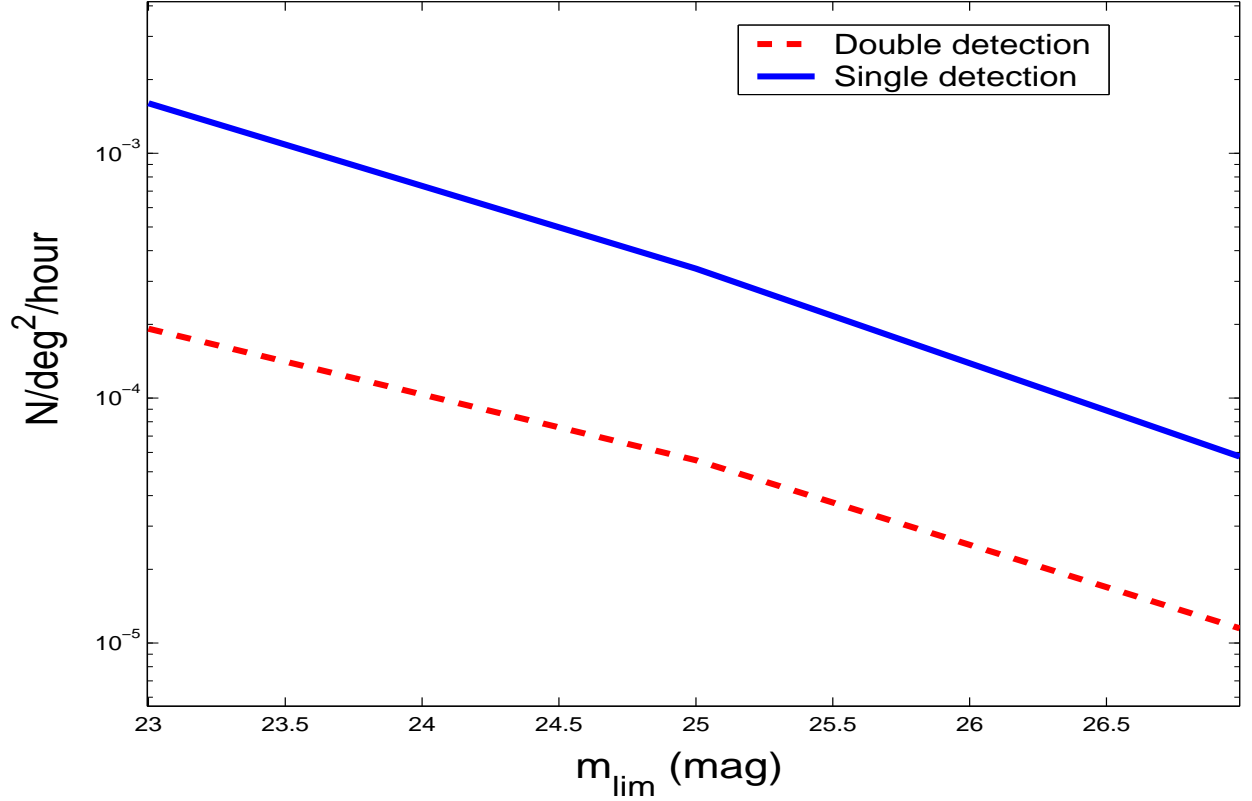


Fig. 5.— The rate of detection of orphan afterglows per square degree per hour of telescope time. The solid curve corresponds to a single detection with our “canonical” normalization ($F_0 = 0.003 \mu Jy$, $z_{peak} = 1$ and $\theta_j = 0.1$). The rate is calibrated for a telescope that reaches $m_{lim} = 25$ in one hour exposure. It can be scaled up or down to other telescopes. The dashed curve corresponds to a double detection (see below) with the same parameters.

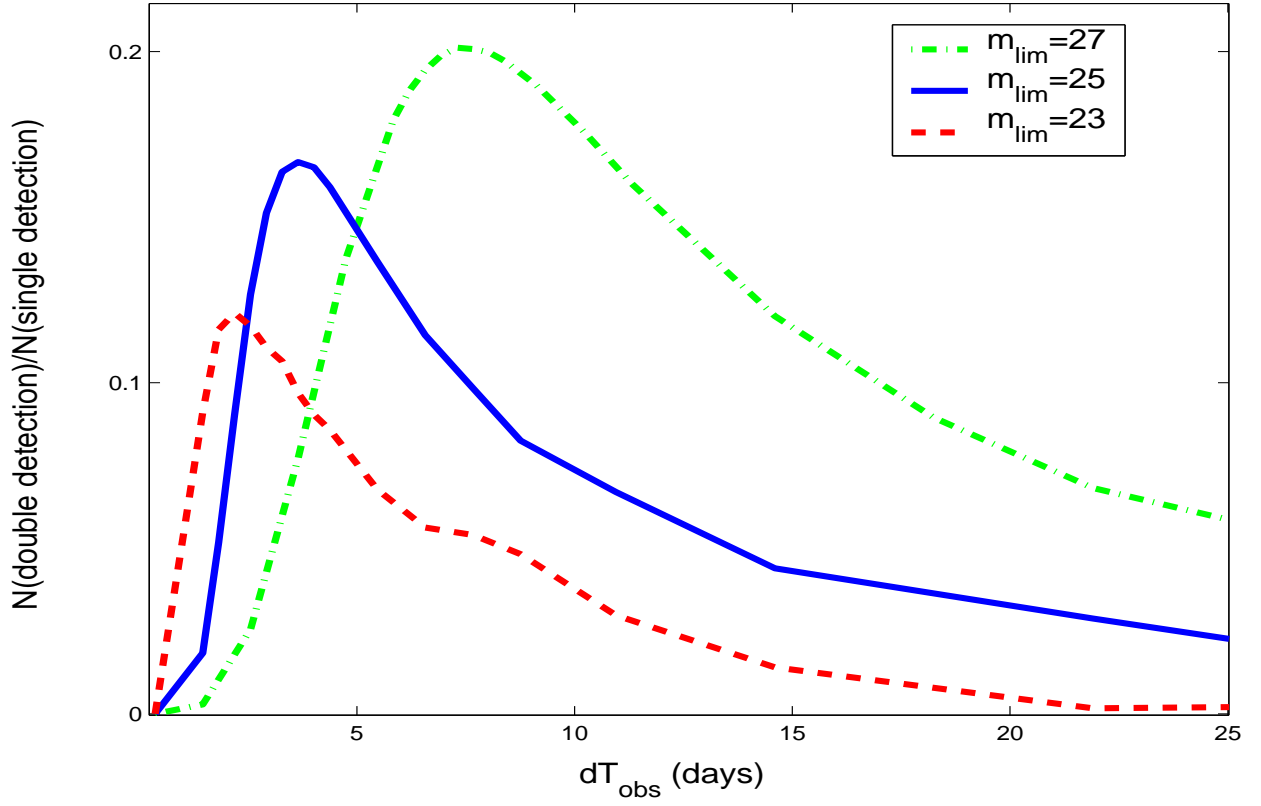


Fig. 6.— The ratio of double detection of orphan afterglows to a single detection as a function of the time delay, dT_{obs} , between the two exposures. The three models are: $F_0 = 0.003 \mu Jy$, $z_{peak} = 1$ and $m_{lim} = 23$ (dashed line) $m_{lim} = 25$ (solid line) and $m_{lim} = 27$ (dashed-dotted line).

Depending on the model the fraction of detected orphan afterglows to the true GRB rate varies from $4 \sim 10^{-3}$ for $m_{lim} = 23$ to $3 \sim 10^{-2}$ for $m_{lim} = 27$ (See Fig 8).

4. Discussion

We have calculated the number per unit solid angle of orphan afterglows that could be detected by idealized surveys with different limiting magnitudes. Our calculations are based on a simple idealized model for the hydrodynamics of the sideways expanding jets. Light curves from other models, including numerical simulations (Granot et al., 2001) described in Granot et al., (2002) show similar behaviour. The normalization factor, F_0 , of this light curve (Eq. 8) is somewhat sensitive to the choice of the model parameters. Even observed afterglows with a clear jet break do not yield a well defined normalization factor, mostly because of uncertainty at their jet-break angles. We estimate that our results for the maximal flux are uncertain by a factor of ~ 10 , corresponding to 2.5 magnitudes. This is translated to an uncertainty by a similar factor in the rate of observed orphan transients (see Fig. 4). However, this uncertainty does not influence the trends that indicate a strategy for optimal orphan afterglow survey.

We stress that we do not consider practical observational issues, such as dust extinction or the ability to identify a weak transient on top of a background host galaxy. We have also assumed idealized weather conditions: when considering a “verified” identification by two successive detections we assumed that a second exposure is always possible. All these factors will reduce the observed rate by some unknown factors below our optimistic values. In some cases we discuss a single detection. By this we mean a single photometric record of a transient in a single snapshot. This is of course a very weak requirement and much more (at least a second detection) would be needed to identify that this was an afterglow.

Finally one should be aware of the possible confusion between orphan afterglows and other transients. Most transients could be completely unrelated (such as supernovae or AGNs) and could be distinguished from afterglows with followup observations. However, there could be a class of related transients like on-axis jets whose gamma-ray emission wasn’t observed due to lack of coverage or failed GRBs. The only quantitative measure that we provide is for the ratio of on-axis afterglows to truly orphan ones.

We have shown that for a given dedicated facility the optimal survey strategy will be to perform many shallow snapshots. However, those should not be too shallow as we will miss all orphan afterglow. A reasonable limiting magnitude will be 25. With this magnitude we should perform a repeated snapshot of the same region after 3 to 4 days.

We consider now several possible surveys. The SDSS (York, 2000) has $m_{lim} \sim 23$ over 10^4 square degrees in the north galactic cap and $m_{lim} = 25$ in the south galactic cap. Fig 4 suggest that under the most optimistic condition we expect 15 detection of orphan afterglow transients in the north galactic cap of the SDSS. A careful comparison of the SDSS sky coverage and the

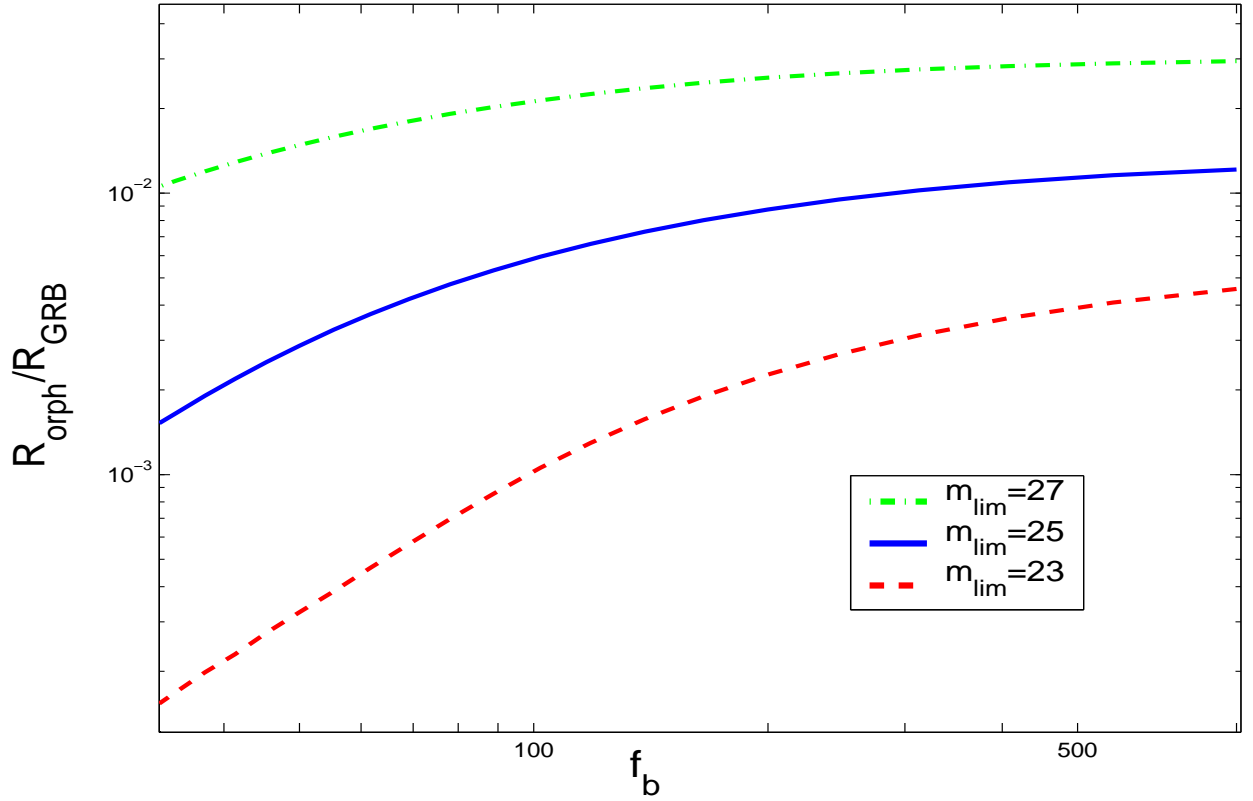


Fig. 7.— The ratio of the rate of orphan afterglows to the true GRB rate ($R_{\text{GRB}}^{\text{true}}$) as a function of the beaming factor. We assume here that we watch all the sky for all the time. The only limit for detection is $m < m_{\text{lim}}$. The three curves are for our “canonical— model ($F_0 = 0.003 \mu\text{Jy}$, $z_{\text{peak}} = 1$, $\theta_j = 0.1$) and $m_{\text{lim}} = 25$ (solid line); $m_{\text{lim}} = 23$ (dashed line) and $m_{\text{lim}} = 27$ (dashed-dotted line).

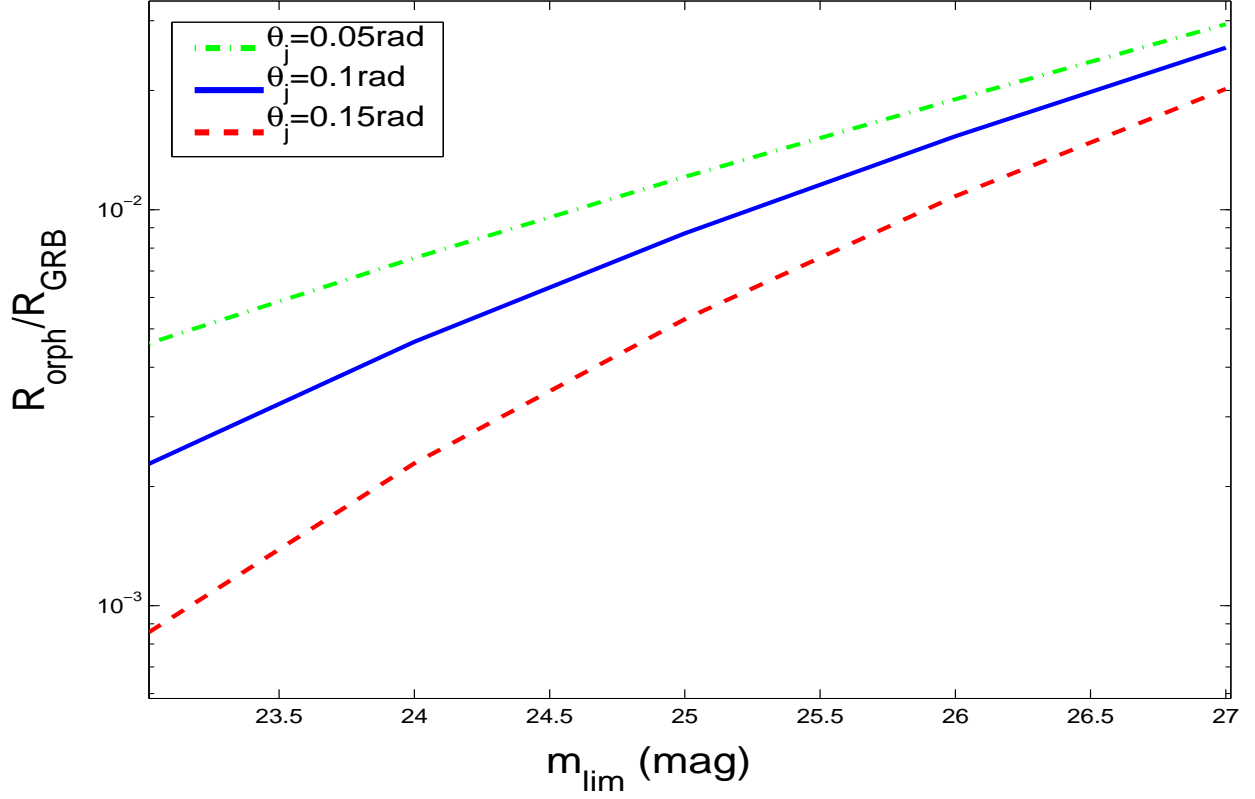


Fig. 8.— The ratio of observed rate of orphan afterglows to the true GRB rate (R_{GRB}^{true}) as a function of m_{lim} . We assume here that we watch all the sky for all the time. The only limit for detection is $m < m_{lim}$. The curves are for our “canonical” model $F_0 = 0.003 \mu Jy$, $z_{peak} = 1$, with $\theta_j = 0.1$ (solid line); $\theta_j = 0.15$ (dashed line) and $\theta_j = 0.05$ (dashed-dotted line).

exposure of relevant GRB satellites could reveal the rate of coincident detection (GRB - Sloan optical transient) from which one could get a better handle (using Table I) on the possible rate of detection of orphan afterglows by SDSS. Under the more realistic assumptions we expect a single orphan afterglow transient in the SDSS. The rate of detection in the more sensitive south galactic cap survey should be comparable as it covers a smaller area which is compensated by the lower threshold.

Consider now a dedicated 2m class telescope with an aperture 0.5° of $m_{lim} = 24$ for a 10 minutes exposure and $m_{lim} = 25$ for a 1 hour exposure. Under our most optimistic assumptions it will record up to 35 orphan afterglows per year in the shallow mode and a third of that (13 afterglows) in the deeper mode. Using our “canonical” model we find two orphan afterglows per year in the shallow mode.

The VIRMOS camera at the VLT has a comparable aperture of 0.5° but it can reach $m_{lim} = 26$ in 10 minutes and $m_{lim} = 27$ in an hour. A single $m_{lim} = 27$ frame would have a 0.02 orphan afterglows under the most optimistic assumptions ($1.1 \cdot 10^{-3}$ canonically). Thus, at best 2 orphan afterglows should be hiding in every 100 exposures. It will be however a remarkable challenge to pick up these transients and confirm their nature from all other data gathered in these 100 exposures.

We thank Tom Broadhurst and Re’em Sari for helpful remarks. This research was supported by a US-Israel BSF grant and by NSF grant PHY-0070928.

REFERENCES

- Bouwenn, E. N. S., Broadhurst, T. J., & Illingworth, R. J., 2002, submitted.
- Dalal, N., Griest, K., & Pruet, J. 2002, ApJ, 564, 209.
- Frail, D. A. et al. 2001, ApJ, 562, L55.
- Granot, J., Miller, M., Piran, T., Suen, W. M., & Hughes, P. A. 2001, Gamma-Ray Bursts in the Afterglow Era, Proceedings of the International workshop held in Rome, CNR headquarters, 17-20 October, 2000. Edited by Enrico Costa, Filippo Frontera, and Jens Hjorth. Berlin Heidelberg: Springer, 2001, p. 312., 312.
- Granot, J., Panaitescu, A., Kumar, P. & Woosley, S. E. 2002, ApJin press, astro-ph/0201322
- Granot, J. & Sari, R. 2002, ApJ, 568, 820.
- Harrison, F. A. et al. 2001, ApJ, 559, 123.
- Harrison, F. A. et al. 1999, ApJ, 523, L121.
- Panaitescu, A. & Kumar, P. 2001, ApJ, 560, L49.

- Piran, T. 1994, AIP Conf. Proc. 307: Gamma-Ray Bursts, 495.
- Piran, T. 2000, Phys. Rep., 333, 529.
- Piran, T., Kumar, P., Panaitescu, A., & Piro, L. 2001, ApJ, 560, L167.
- Rhoads, J. E. 1997, ApJ, 487, L1.
- Rhoads, J. E. 1999, ApJ, 525, 737.
- Sari, R., Piran, T., & Narayan, R. 1998, ApJ, 497, L17.
- Sari, R., Piran, T., & Halpern, J. P. 1999, ApJ, 519, L17.
- Stanek, K. Z., Garnavich, P. M., Kaluzny, J., Pych, W., & Thompson, I. 1999, ApJ, 522, L39.
- York, D. G. et al. 2000, AJ, 120, 1579.